Journal of Alloys and Compounds 655 (2016) 353–356

Contents lists available at ScienceDirect

Journal of Alloys and Compounds

journal homepage: http://www.elsevier.com/locate/jalcom

Achieving an enhanced magneto-caloric effect by melt spinning a $Gd_{55}Co_{25}Al_{20}$ bulk metallic glass into amorphous ribbons

P. Yu, N.Z. Zhang, Y.T. Cui, L. Wen, Z.Y. Zeng, L. Xia*

Chongqing Key Laboratory of Photo-Electric Functional Materials, College of Physics and Electronic Engineering, Chongqing Normal University, Chongqing, 401331, China

A R T I C L E I N F O

Article history:
Received 8 July 2015
Received in revised form
19 September 2015
Accepted 22 September 2015
Available online 25 September 2015

Keywords:
Metallic glass
Magneto-caloric effect
Magnetic entropy change

A B S T R A C T

The magneto-caloric effect (MCE) and microstructure of the $Gd_{55}Co_{25}Al_{20}$ metallic glasses were studied in the present work. It was found that the amorphous ribbons exhibit a peak value of magnetic entropy change ($-\Delta S_m^{peak}$) up to 39.5% higher than that of the bulk metallic glass (BMG) under a magnetic field of 1 T. The mechanism for the enhanced MCE of amorphous ribbons was investigated and the dependence of magneto-caloric behaviors on the microstructure of the glassy alloys was revealed. The larger $-\Delta S_m^{peak}$ as well as refrigeration capacity under low magnetic field, together with the higher heat exchange efficiency of the ribbons, indicates that the amorphous ribbons could be more suitable candidates as the magnetic refrigerants rather than the BMG.

1. Introduction

The magneto-caloric effect (MCE), referred to the heating or cooling of a magnet with the variation of a magnetic field, was firstly discovered by Warburg in 1881 [1,2]. With the rising concerns on global warming and the ever increasing global consumption of energy in recent years, MCE has attracted intensive interests due to their promising application potential in magnetic refrigeration (MR) technology, which can have a potential energy saving of 30% compared to the conventional vapor compression technique and can avoid using ozone-depleting gases [2–10]. Therefore, as the working materials of the MR technology, a lot of materials with excellent MCE have been developed in the last decades [11–36].

Among these materials, the amorphous alloys seems to be ideal candidates for magnetic refrigerants because of their ultrahigh refrigeration capacity (*RC*) resulted from their broadened magnetic entropy change *vs* temperature ($(-\Delta S_m)$-T) curve, low energy loss due to their large electric resistance and nearly zero magnetic hysteresis, better corrosion resistance and mechanical properties than their crystalline counterparts corresponding to their unique disordered structures [22–36]. However, the broadened $-\Delta S_m$ peaks of the amorphous alloys not only result in the high *RC* but also cause a relatively lower peak value of the magnetic entropy change ($-\Delta S_m^{peak}$) and a resultant lower adiabatic temperature rise (ΔT_{ad}), while both the large *RC*, the high $-\Delta S_m^{peak}$ and the large ΔT_{ad} are the principal features of the magneto-caloric materials with high refrigeration efficiency. Although the $-\Delta S_m^{peak}$ values of recently developed Gd-based bulk metallic glasses (BMGs) are comparable to those of the crystalline alloys that undergo a second order magnetic phase transition, they are still much lower than the $-\Delta S_m^{peak}$ values of intermetallic compounds that undergo a first order magnetic phase transition [11–21]. Therefore, the key issue for the industrial use of these amorphous alloys is how to further improve their $-\Delta S_m^{peak}$ and ΔT_{ad}.

The commonly used way to improve the $-\Delta S_m^{peak}$ of the amorphous alloys is to adjust the composition of the alloys. For example, we have improved the $-\Delta S_m^{peak}$ of $Gd_{55}Co_{25}Al_{20}$ BMG by minor addition of Zn and Ni [32,34], and $-\Delta S_m^{peak}$ of Fe–Zr–B ternary amorphous alloys can be obviously improved by Mn, Cr and Co additions [36]. More recently, it was found that the $-\Delta S_m^{peak}$ of the amorphous alloys has been obviously improved by fabricating the BMG into the shape of ribbons or wires [29,33]. However, the mechanism for the enhanced $-\Delta S_m^{peak}$ of amorphous ribbons/wires was not very clear till now. In the present work, we prepared the $Gd_{55}Co_{25}Al_{20}$ amorphous ribbons by melt-spinning and obtained larger $-\Delta S_m^{peak}$ and *RC* in the $Gd_{55}Co_{25}Al_{20}$ amorphous ribbons than in the BMG. The $(-\Delta S_m)$-T curves under different magnetic field were constructed from the isothermal magnetization curves of $Gd_{55}Co_{25}Al_{20}$ amorphous ribbons. The field dependence of $-\Delta S_m^{peak}$

* Corresponding author.
E-mail address: xialei@cqnu.edu.cn (L. Xia).

http://dx.doi.org/10.1016/j.jallcom.2015.09.205
0925-8388/

($-\Delta S_m^{peak}$-H curve) of the as-spun $Gd_{55}Co_{25}Al_{20}$ ribbons was constructed and compared to that of the as-cast $Gd_{55}Co_{25}Al_{20}$ rod. The different magneto-caloric behaviors between the amorphous ribbons and their bulk counterpart were revealed and the mechanism for the improved $-\Delta S_m^{peak}$ was studied.

2. Experiments

An $Gd_{55}Co_{25}Al_{20}$ ingot was prepared by arc-melting 99.9% (at.%) pure Gd, Co and Al under a titanium-gettered argon atmosphere. As-cast rods of 2 mm diameter were synthesized by copper mold suction casting under an argon atmosphere; as-spun ribbons, about 40 μm in thickness, were prepared by a single copper wheel with a surface speed of about 20 m/s under a pure argon atmosphere. The structure of the rods and ribbons was characterized by the X-ray diffraction (XRD) on a Rigaku D\max−2550 diffractometer using Cu K_α radiation. The microstructural investigation of the amorphous samples was performed on a JEOL JEM−2010F high resolution electron microscope (HREM). Specimen for HREM observation were prepared by ion-polishing under a pure argon atmosphere using the GATAN 691 precision ion-polishing system. The magnetic properties of the amorphous samples were measured by a Quantum Design Physical Properties Measurement System (PPMS 6000): from 10 K to 300 K under a field of 0.03 T for the temperature dependence of magnetization (*M-T*) curve; for the hysteresis loops, at 10 K and 300 K respectively under the field of 2 T; for the isothermal magnetization (*M-H*) curves, from 60 K to 200 K with a temperature step of 5 K and a magnetic field step of 0.01 T under a field of 5 T.

3. Results and discussion

Fig. 1 shows the XRD patterns and the HREM images of the $Gd_{55}Co_{25}Al_{20}$ as-cast rod and as-spun ribbon, respectively. The typical broad diffraction maxima in the XRD patterns of both the as-cast rod and the as-spun ribbons indicate the amorphous features of amorphous phases. However, HREM images have revealed that the as-spun ribbon is of typical amorphous characteristics with numerous short range order (SRO), while the as-cast rod contains nano-crystallite (NC) and medium range order (MRO) on the amorphous matrix.

The hysteresis loops of the $Gd_{55}Co_{25}Al_{20}$ as-spun ribbons measured at 10 K and room temperature under a field of 2 T are shown in Fig. 2 (a). The ribbons is paramagnetic at room temperature and is soft magnetic at 10 K with a saturation magnetization (M_s) of about 203 Am^2/kg and a nearly zero coercivity (less than 5 kA/m, as shown in the lower right inset of Fig. 2(a), a zoom of the *M-H* curve around zero magnetic field). The Curie temperature (T_c) obtained from the derivative of the *M-T* curve of the $Gd_{55}Co_{25}Al_{20}$ as-spun ribbons, as shown in the upper left inset of Fig. 2 (a), is about 112.5 K. The paramagnetic moment obtained from the *M-T* curve of the $Gd_{55}Co_{25}Al_{20}$ as-spun ribbons is about 0.7 μ_B according to the Curie−Weiss law. The M_s and T_c of the amorphous ribbons are roughly in accordance with those of the BMG within the detection error limit [27].

Fig. 2 (b) shows the isothermal magnetization curves of the $Gd_{55}Co_{25}Al_{20}$ amorphous ribbons measured from 60 K to 200 K under a field of 5 T. Therefore, the($-\Delta S_m$)-T curves for the amorphous ribbons under different magnetic field, as shown in Fig. 3 (a), can be derived from these *M-H* curves according to the thermodynamic Maxwell equation

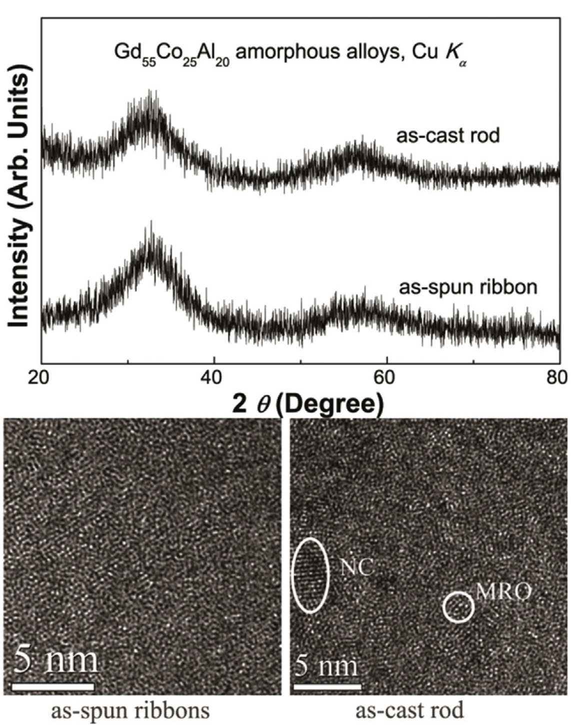

Fig. 1. XRD patterns and HREM images of the $Gd_{55}Co_{25}Al_{20}$ as-cast rod and as-spun ribbons.

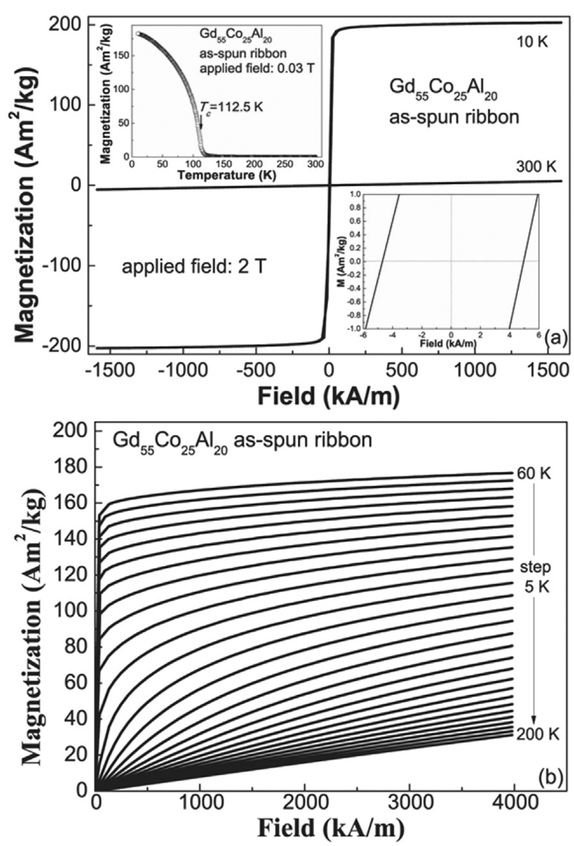

Fig. 2. (a) Magnetic hysteresis loops of the $Gd_{55}Co_{25}Al_{20}$ as-spun ribbons at 10 K and 300 K under a magnetic field of 2 T, the upper left inset shows the *M-T* curve of the amorphous ribbons and the lower right inset shows the zoom of the hysteresis loop at low field; (b) *M-H* curves for the $Gd_{55}Co_{25}Al_{20}$ as-spun ribbons from 60 K to 200 K under a magnetic field of 5 T.